Supporting information

Isothermal amplification-mediated lateral flow biosensors for *in vitro* diagnosis of gastric cancer-related microRNAs

Seung Beom Seo[a,b], Jin-Seong Hwang[c,d], Eunjung Kim[e,f], Kyujung Kim[b], Seokbeom Roh[g,h], Gyudo Lee[g,h], Jaewoo Lim[a,i], Byunghoon Kang[a], Soojin Jang[a,i], Seong Uk Son[a,i], Taejoon Kang[a], Juyeon Jung[a], Jang-Seong Kim[c,d], Keun-Hur[j], Tae-Su Han[c,d] and Eun-Kyung Lim[a,i,]**

[a]Bionanotechnology Research Center, Korea research institute of bioscience and biotechnology (KRIBB), Daejeon, 34141, Republic of Korea

[b]Department of Cogno-Mechatronics Engineering, Pusan National University, Pusan 46241, Republic of Korea

[c]Biotherapeutics Translational Research Center, KRIBB, Daejeon, 34141, Republic of Korea

[d]Department of Functional Genomics, KRIBB School of Biotechnology, University of Science and Technology (UST), Daejeon 34113, Republic of Korea

[e]Department of Bioengineering & Nano-bioengineering, Incheon National University, Incheon 22012, Republic of Korea

[f]Division of Bioengineering, Incheon National University, Incheon 22012, Republic of Korea

[g]Department of Biotechnology and Bioinformatics, Korea University, Sejong 30019, Republic of Korea

[h]Interdisciplinary Graduate Program for Artificial Intelligence Smart Convergence Technology, Korea University, Sejong 30019, Republic of Korea

[i]Department of Nanobiotechnology, KRIBB School of Biotechnology, UST, Daejeon 34113,

Republic of Korea

[j]Department of Biochemistry and Cell Biology, School of Medicine, Kyungpook National University, Daegu 41944

[*]**Corresponding authors**

Eun-Kyung Lim. E-mail: eklim1112@kribb.re.kr

Tae-Su Han. Tel E-mail: tshan@kribb.re.kr

Experimental section

Rolling circle amplification (RCA)-based isothermal amplification for miRNA detection in solution

The ligation reaction was performed in 30 μL of a reaction mixture containing diethylpyrocarbonate (DEPC)-treated water, various target DNA concentrations, and 5 μL of circular DNA at 55 °C for 5 min, followed by immediate cooling to 37 °C for 1 h. The RCA reaction was conducted at 37 °C in a final volume of 40 μL containing 1× phi29 DNA polymerase buffer (50 mM Tris-HCl (pH 7.5), 10 mM $MgCl_2$, 10 mM $(NH_4)_2SO_4$, and 4 mM dithiothreitol), phi29 DNA polymerase (0.5 μL; 10 U/μL), and dNTPs (0.4 μL; each 2.5 mM) for 2 h. Enzymes were inactivated by incubating the reaction mixture at 65 °C for 10 min. Next, the resulting mixture was incubated with the reporter probe (0.5 nM) at 37 °C for 30 min.

Table S1. Sequences of rolling circle amplification probes.

Name	Sequence (5′ → 3′)
Target DNA (miRNA-135b)	TAT GGC TTT TCA TTC CTA TGT GA
Oncogene (miRNA-21)	TAG CTT ATC AGA CTG ATG TTG A
Padlock probe (miRNA-135b)	P – ***TGA AAA GCC ATA*** CAA ACA ACC CCA ATA CAA CAA CAG ***TCA CAT AGG AA***
Padlock probe (miRNA-21)	P – ***CTG ATA AGC TA***C AAA CAA CCC CAA TAC AAC AAC AG***T CAA CAT CAG T***
Capture probe (miRNA-135b)	TGA AAA GCC ATA - (T10) - [B]
Capture probe (miRNA-21)	CTG ATA AGC TA - (T10) - [B]
Detection probe	F – CAA ACA ACC CCA ATA C

*** P indicates 5′ phosphate modification; T indicates 3′ thymine (T10) modification.**

*** Underline indicates signal primer sequence.**

*** Bold and italic characters indicate sequences complementary to the target and capture probe, respectively.**

*** F indicates 5′ FAM modification; B indicates 3′ biotin modification.**

Probe pair	Circular DNA	Capture probe (CP) + Target (T)	CP + T + Circular DNA
miRNA-135b	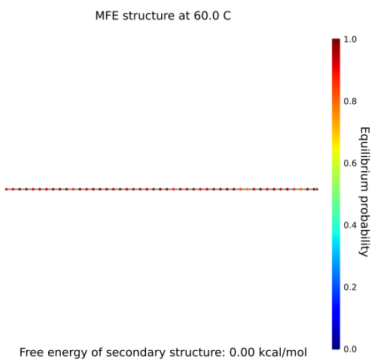	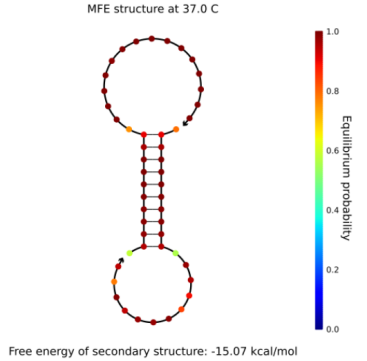	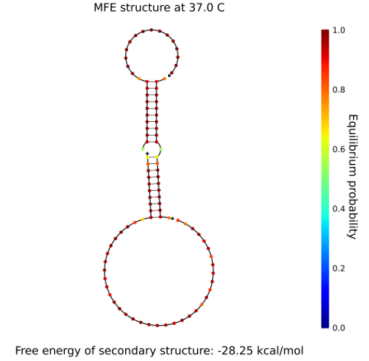
miRNA-21	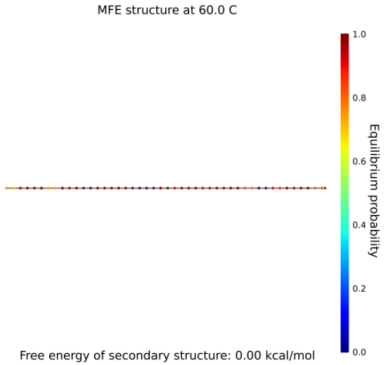	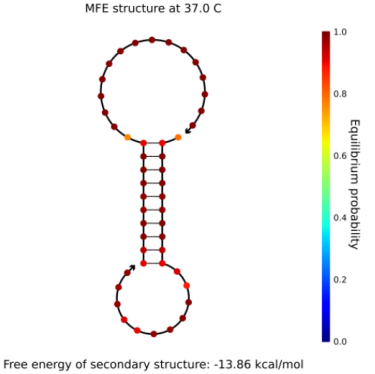	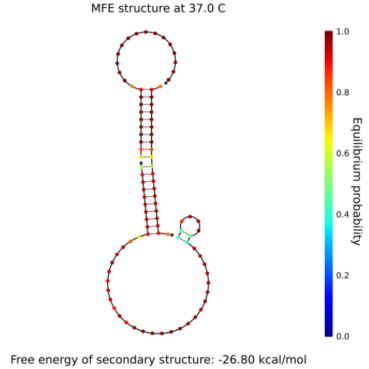

Figure S1. Alignment and thermodynamic properties of the DNA probe in the diagnostic system reported by Nucleic Acid Package (NUPACK). Confirmation of binding force between circular DNA and target and probe. No secondary structures were formed between the circular DNA and target miRNAs at 60 °C (i, iv). The capture probe (CP) and target miRNAs show a strong binding force at 37 °C (ii, v). Confirmation of the binding possibility of target miRNAs and circular DNA bound to CP at 37 °C (iii, vi). The sequence concentration input to the NUPACK software is the same as the experimental condition.

Table S2. Sequences of microRNAs used as negative controls.

	Sequence (5′ → 3′)
miRNA-103-3p	AGCAGCATTGTACAGGGCTATGA
miRNA-143-3p	TGAGATGAAGCACTGTAGCTC
miRNA-365-5p	AGGGACTTTTGGGGGCAGATGTG
miRNA-30e-5p	TGTAAACATCCTTGACTGGAAG
miRNA-342-3p	TCTCACACAGAAATCGCACCCGT
miRNA-574-5p	TGAGTGTGTGTGTGTGAGTGTGT
Let-7i	TGAGGTAGTAGTTTGTGCTGTT
miRNA-21	TAGCTTATCAGACTGATGTTGA
miRNA-135b	TATGGCTTTTCATTCCTATGTGA

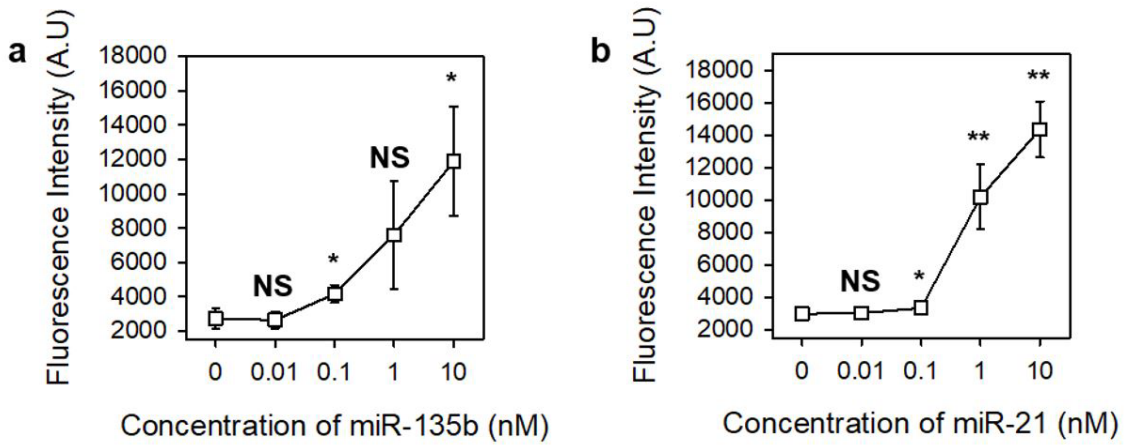

Figure S2. Evaluation of the sensitivity of the rolling circle amplification-based isothermal amplification reaction to detect microRNAs (miRNAs) in solution. (a, b) The graph shows the fluorescence intensity of various concentrations of target miRNAs. The test concentrations of target miRNAs were (i) 0, (ii) 0.01, (iii) 0.1, (iv) 1, and (v) 10 nM. Sensitivity tests for (a) miRNA-135b and (b) miRNA-21 were performed. Error bars represent the standard deviation of triplicate tests. NS, non-significance.

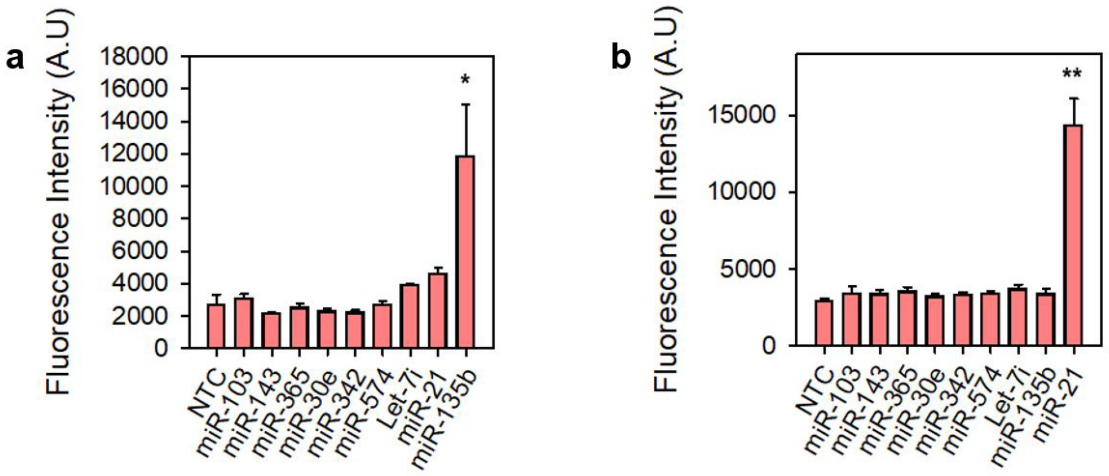

Figure S3. Evaluation of the specificity of the rolling circle amplification-based isothermal amplification reaction to amplify microRNAs (miRNAs) in solution. (a, b) Target selectivity was confirmed using eight types of miRNAs as controls. Selectivity tests for (a) miRNA-135b and (b) miRNA-21 were performed. Error bars represent the standard deviation of triplicate tests.

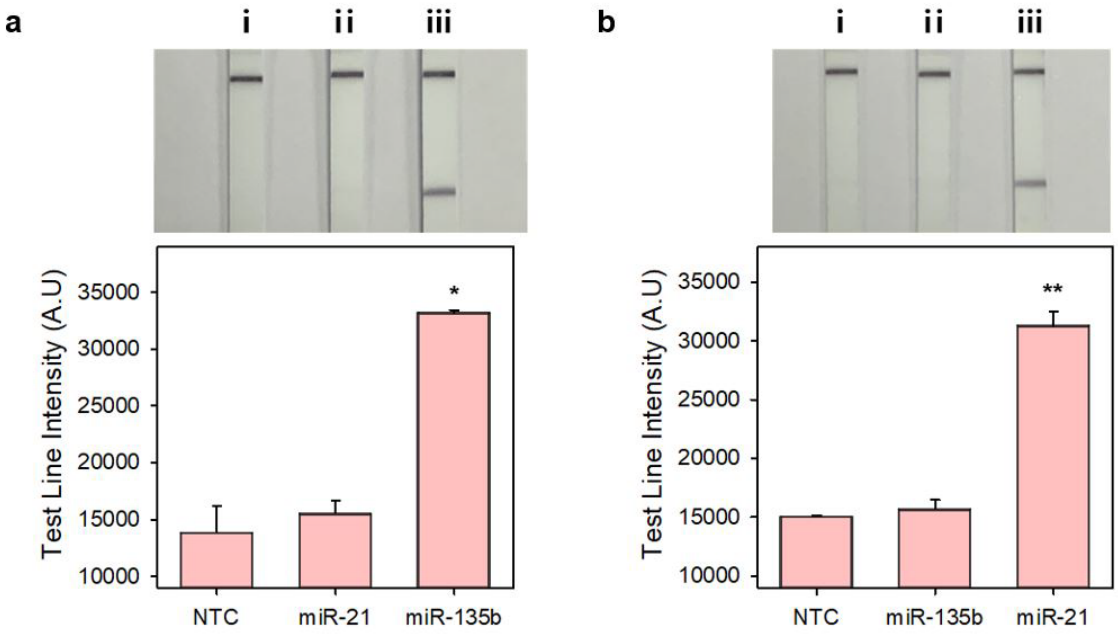

Figure S4. Cross-validation of the amplification of target microRNAs (miRNAs) using an isothermal amplification-based lateral flow biosensor (IA-LFB). (a, b) Cross-validation of the ability of IA-LFB to detect (a) miRNA-135b and (b) miRNA-21. Error bars represent the standard deviation of triplicate tests.

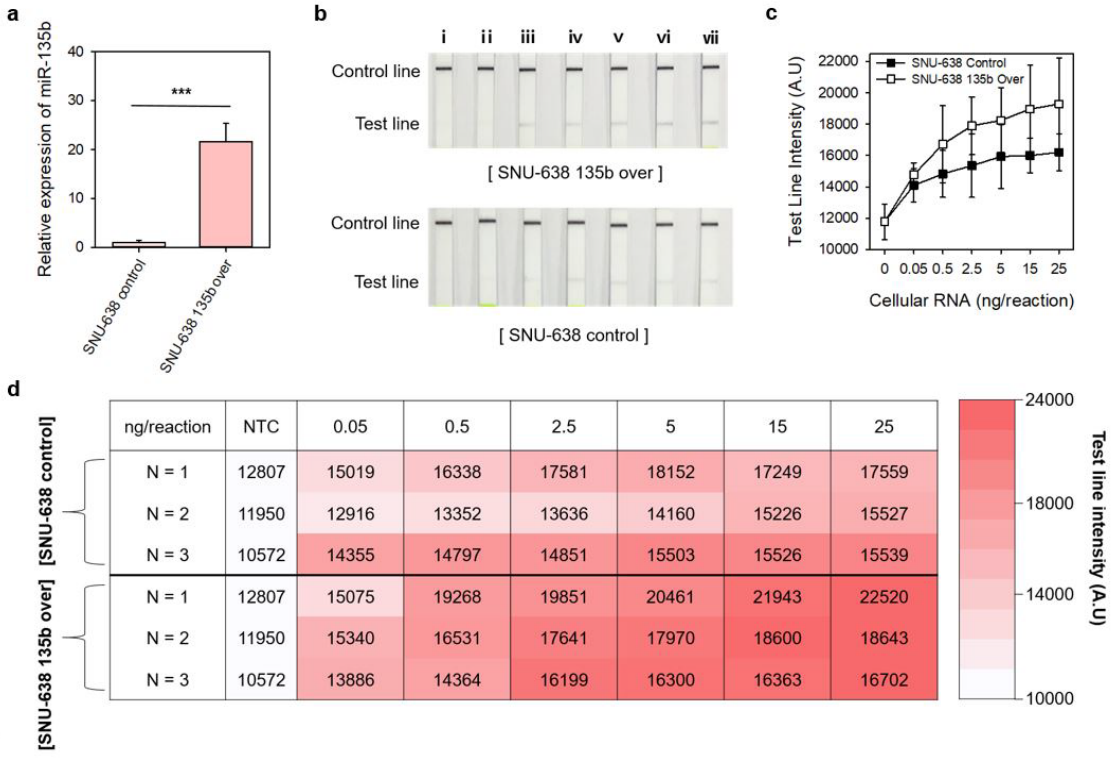

	ng/reaction	NTC	0.05	0.5	2.5	5	15	25
[SNU-638 control]	N = 1	12807	15019	16338	17581	18152	17249	17559
	N = 2	11950	12916	13352	13636	14160	15226	15527
	N = 3	10572	14355	14797	14851	15503	15526	15539
[SNU-638 135b over]	N = 1	12807	15075	19268	19851	20461	21943	22520
	N = 2	11950	15340	16531	17641	17970	18600	18643
	N = 3	10572	13886	14364	16199	16300	16363	16702

Figure S5. Evaluation of miRNA-135b detection sensitivity of the isothermal amplification-based lateral flow biosensor (IA-LFB) in cellular RNA samples extracted from *in vitro* samples. (a) Comparative analysis of the relative expression levels of miRNA-135b in RNA samples extracted from miRNA-135b-overexpressing SNU-638 (SNU-638 135b over) and control SNU-638 cells using quantitative real-time polymerase chain reaction. (b, c) The test concentrations of cellular RNA were (i) 0, (ii) 0.05, (iii) 0.5, (iv) 2.5, (v), (vi) 15, and (vii) 25 ng per reaction. NTC, no template control. (d) A heat-map showing the test line intensity values according to the concentration of RNA extracted from SNU-638 135b over and control SNU-638 cells. Error bars represent the standard deviation of triplicate tests.

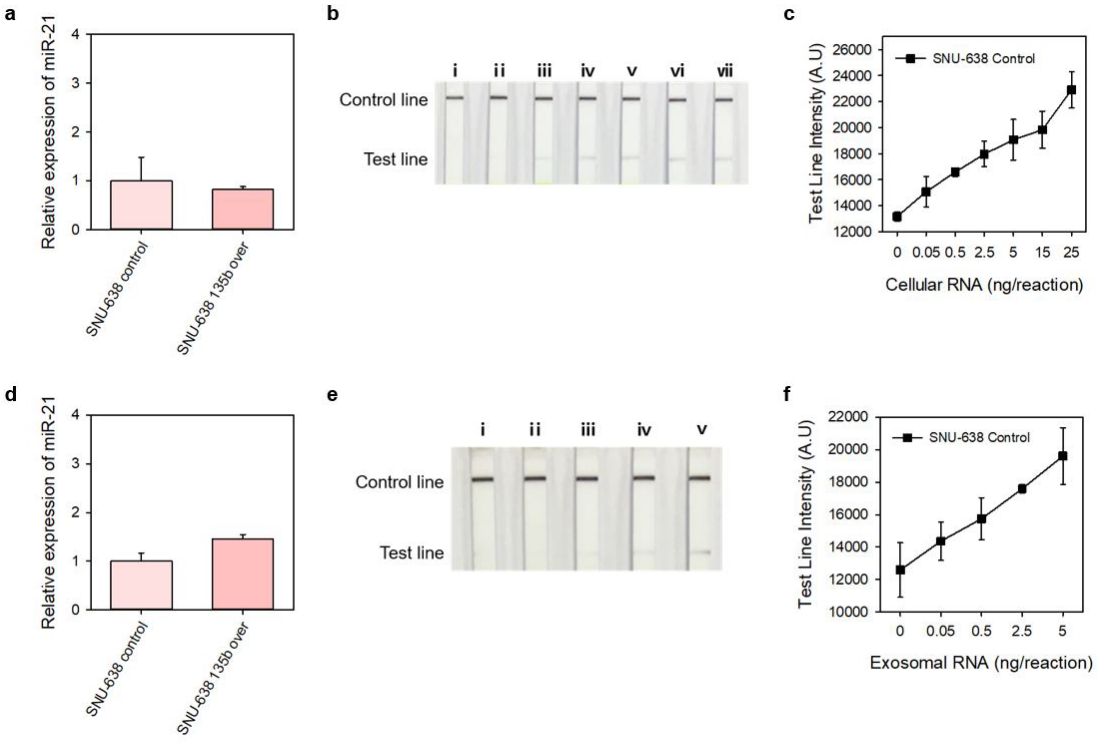

Figure S6. Evaluation of miRNA-21 detection sensitivity of isothermal amplification-based lateral flow biosensor (IA-LFB) in RNA samples isolated from *in vitro* samples. Comparative analysis of the relative expression levels of (a) cellular miRNA-21 and (d) exosomal miRNA-21 in RNA samples extracted from control SNU-638 cells using quantitative real-time polymerase chain reaction. Ability of IA-LFB to detect miRNA-21. The test concentrations of RNAs extracted from cells were (i) 0, (ii) 0.05, (iii) 0.5, (iv) 2.5, (v) 5, (vi) 15, and (vii) 25 ng per reaction. (b–c: cellular RNA and e–f: exosomal RNA). (b and e) The image of IA-LFB after miRNA-21 detection and (c and f) the intensity of test lines. NTC, no template control. Error bars represent the standard deviation of triplicate tests.

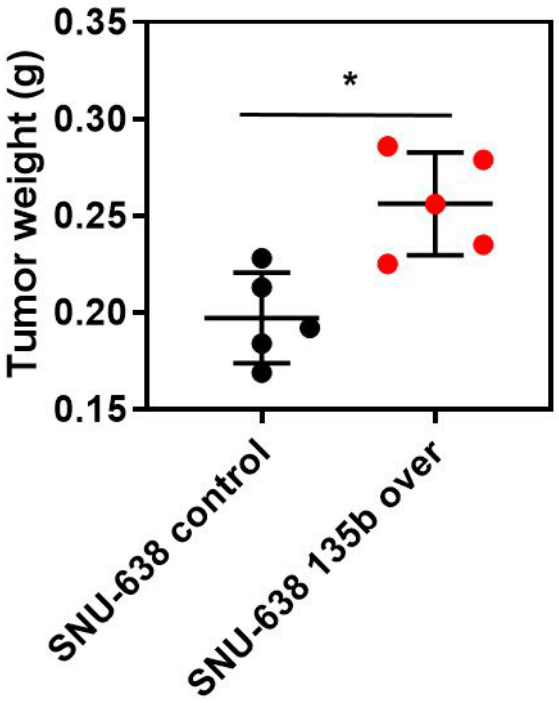

Figure S7. Weight of tumors excised from xenograft mouse models. Weights of tumors from mouse gastric cancer xenograft models injected with SNU-638 control and miRNA-135b-overexpressing SNU-638 cells (SNU-638 135b over). Five mice were tested for each group. Each circle indicates the weight of individual tumors (black: SNU-638 cell-derived tumors and red: SNU-638b 135b over cell-derived tumors). The line graph shows the average and standard deviation.

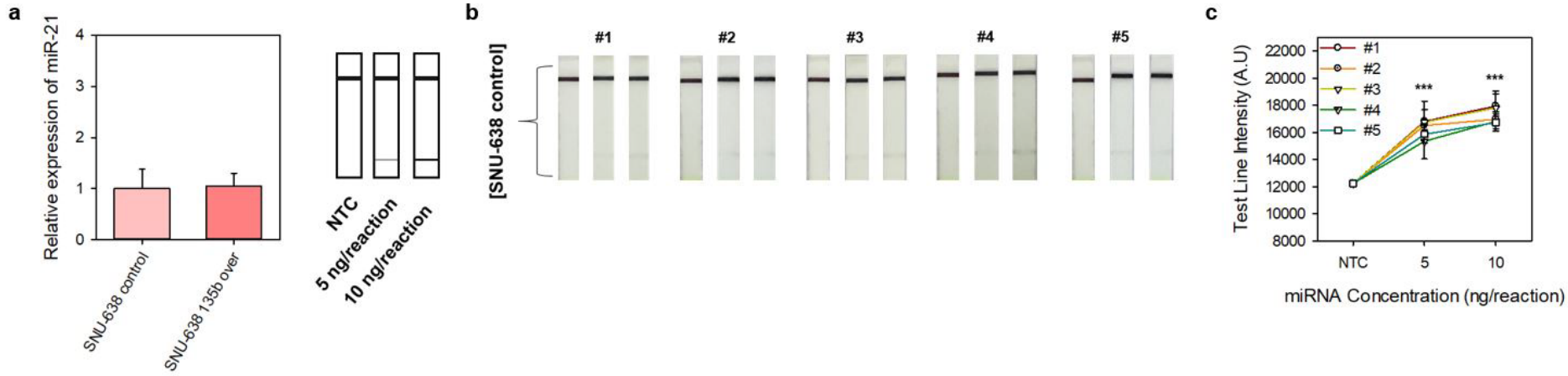

Figure S8. Evaluation of the miRNA-21 detection ability of the isothermal amplification-based lateral flow biosensor (IA-LFB) using RNA samples extracted from *in vivo* models. (a) Comparative analysis of the relative expression levels of miRNA-21 in RNA samples extracted from *in vivo* models using quantitative real-time polymerase chain reaction. (b) The images of IA-LFB after detection of miRNA-21 in RNA samples extracted from control SNU-638 cell-injected tumors and (c) the test line intensities. The test RNA concentrations were 0, 5, and 10 ng per reaction. Error bars represent the standard deviation of triplicate tests.